Characterization of Electrochromic Devices by Phase Modulated Spectroscopic Ellipsometry

C. Eypert, HORIBA Jobin Yvon SAS, Thin Film Division, Chilly-Mazarin, France;
and L. Yan and E. Teboul, HORIBA Jobin Yvon Inc., Thin Film Division, Edison, NJ

ABSTRACT

The performance of an electrochromic (EC) switching device is directly related to the optical properties and physical dimensions of the layers constituting the device. Accurate characterizations of the individual layers in an EC device are thus vital to predicting the device performance. In this work, we present ellipsometric results obtained by a phase modulated spectroscopic ellipsometer (PMSE) on a complete electrochromic device: Glass/ITO/$TiVO_x$/Ta_2O_5/WO_3/ITO/Glass. To characterize accurately all the materials present in the device, five separate samples with step-wise layer constructions were measured. Depending on the optical responses of the materials, several dispersion formulae were used accordingly: 1) Lorentzian oscillators plus a Drude edge for ITO, 2) new amorphous for both WO_3 and $TiVO_x$, and 3) absorbing Lorentz for Ta_2O_5. Results from the five measured samples showed the clear evolutions of the properties of the layers with their surroundings in a multi-layered stack. These measurements were made possible owing to the extremely high accuracy and sensitivity of PMSE in measuring multiple thin films on transparent substrates.

INTRODUCTION

Electrochromic (EC) devices operate in such that an incoming electromagnetic radiation is modulated via transmission, absorption, or reflection of the light. This is accomplished through the application of an external electric field across the device. At the heart of an EC device are electrochromic materials, organic or inorganic, which can interconvert between two or more color states upon oxidation or reduction; i.e., upon electrolytic loss or gain of electrons [1]. Listed under smart chromogenic systems, EC materials are quickly finding their niches in various applications; e.g., electrochromic smart windows, anti-dazzling rear view mirrors, switchable motorcycle helmets, in some emissive display devices for contrast enhancement, and in non-emissive large area color displays for information advertisement. Despite numerous studies in seeking its alternatives, tungsten oxide (WO_3) has remained thus far the most commonly used electrochromic chemical (especially in the smart window systems) due to its high coloration efficiency and long-term cyclability [1-3]. The material switches reversibly from white/yellow to blue upon electrochemical oxidation and reduction [4-5].

A typical absorptive/transmissive-type electrochromic device is a sandwich-like structure with two glass plates and an electrolyte, as shown in Figure 1. Each glass plate is coated on the inside with a transparent electrically conducting layer of (typically) indium tin oxide (ITO) as an electrode for charge (ion) insertion/extraction. One of the electrodes must be coated with an electrochromic material (usually WO_3); whereas the other can have deposited either another EC material with complementary properties or, an ion storage layer (stock layer) which remains transparent upon charge insertion.

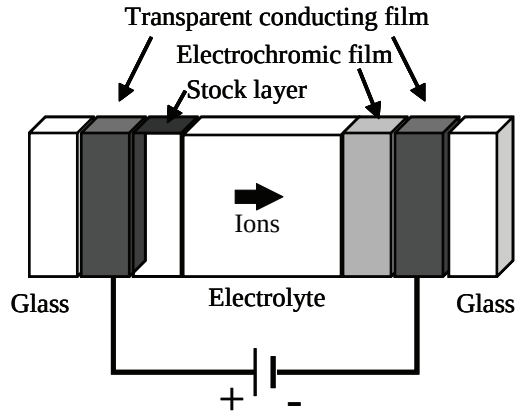

Figure 1: Schematic of an absorptive/transmissive-type electrochromic device.

The performance of an EC device is directly related to the optical properties and physical dimensions of the materials constituting the EC structure. As such, accurate characterizations of each of the individual layers in an EC device are critical to predicting the device performance. Spectroscopic ellipsometry (SE) is a well-known surface sensitive, non-destructive, relatively low-cost optical technique widely used to determine film thickness and optical constants [6,7]. Reflection ellipsometry measures the change of polarization state of light upon reflection from a sample surface. The two traditional ellipsometric angles, Ψ and Δ, are respectively the ratios of the amplitude and phase changes for the p- and s-components of polarized light, and are related to the complex Fresnel reflection coefficients (R) of the sample as follows:

$$\rho \equiv \tan\Psi e^{i\Delta} = \frac{R_p}{R_s} \quad (1)$$

 505/856-7188
50th Annual Technical Conference Proceedings (2007) ISSN 0737-5921

where p- and s- correspond to directions parallel and perpendicular to the plane of incidence, respectively.

As ellipsometry is an indirect technique, a modeling-based analysis procedure is thus required to extract film thickness, optical constants, as well as other interested materials properties; e.g., composition, anisotropy, crystallinity, and roughness, etc. With initial estimates for the unknown layer thickness and/or optical constants, a set of Ψ and Δ values are calculated for the known wavelengths and angles of incidence. The weighted Chi-Square (χ^2) residual value,

$$\chi^2 = \min \sum_{i=1}^{n} \left[\frac{(\Psi_{th} - \Psi_{\exp})_i^2}{\Gamma_{\Psi,i}} + \frac{(\Delta_{th} - \Delta_{\exp})_i^2}{\Gamma_{\Delta,i}} \right] \quad (2)$$

which quantifies the difference between measured and model generated values, is then minimized using the Levenberg–Marquardt algorithm.

In this work, we present ellipsometric results obtained by a phase modulated spectroscopic ellipsometer (PMSE) on a complete electrochromic device: Glass/ITO/ Titanium-Vanadium oxide ($TiVO_x$)/Tantalum pentoxide (Ta_2O_5)/WO_3/ITO/Glass. $TiVO_x$ and Ta_2O_5 perform as a second electrochromic (complementary to WO_3) and the electrolyte materials, separately. Compared to conventional rotating element ellipsometers, PMSE features high-accuracy determination of the ellipsometric angles (Ψ, Δ) across their full ranges, thus allowing superior precision and sensitivity for the characterization of transparent substrates, ultra-thin films and films with low index contrast. The three measurable of PMSE are Is, Ic, and Ic', which are related to Ψ and Δ by:

$$I_s = \sin 2\Psi \sin \Delta$$
$$I_c = \sin 2\Psi \cos \Delta$$
$$I_c^{'} = \cos 2\Psi \quad (3)$$

EXPERIMENTAL

In an effort to characterize with the best accuracy the individual layers constituting the device, five separate samples with stepwise layer constructions were measured: (1) Glass/ITO, (2) Glass/ITO/WO_3, (3) Glass/ITO/$TiVO_x$, (4) Glass/ITO/$TiVO_x$/Ta_2O_5, and (5) Glass/ITO/$TiVO_x$/Ta_2O_5/WO_3.

The ellipsometry system used for this study was the UVISEL phase modulated spectroscopic ellipsometer manufactured by HORIBA Jobin Yvon SAS. Details on this system have been elaborated elsewhere [8]. Briefly, after passing through the first polarizer which establishes a linear polarization, the probing beam from the Xenon arc source reflects at an oblique angle from the sample surface. The output head comprises a 50kHz photoelastic modulator (PEM) and an analyzing polarizer that resolves the polarization state of the reflected beam. The PEM is a rectangular shaped fused silica cemented with a piezoelectric quartz crystal. When activated via a 50kHz sinusoidal signal, it introduces a periodic relative phase shift between orthogonal components of the transmitted beam. Following the output head is a high-resolution grating monochromator which directs sequentially the light for each wavelength onto the detector. Two types of detectors are employed: photomultiplier for the far UV-VIS region and InGaAs photodiodes for the near infrared (NIR) extension. A combo data acquisition and digital signal processing board is used to process modulated signal.

In this work, ellipsometric data were collected at an angle of incidence of 70° using the UVISEL NIR which covers a spectral range from 260 to 2100 nm. The full electrochromic device characterization was carried out successfully over the spectral range of 1-4 eV (1240-310 nm).

RESULTS AND DISCUSSIONS

The analysis strategy was to break down a complete electrochromic device into separate samples, with the individual layers added on in a step-wise fashion. This rendered a close-up investigation of each constituent material and as such the evolutions of their optical properties (if any) with the surroundings in a multi-layered structure.

3.1. Glass/ITO

The optical responses of ITO were described using an empirical function called Classical oscillator model:

$$\varepsilon = \underbrace{\varepsilon_\infty}_{\text{High frequency } \varepsilon} + \underbrace{\frac{(\varepsilon_s - \varepsilon_\infty)\omega_t^2}{\omega_t^2 - \omega^2 + i\Gamma_o\omega}}_{\text{Lorentz oscillator}} + \underbrace{\frac{\omega_p^2}{-\omega^2 + i\Gamma_D\omega}}_{\text{Drude oscillator}} + \underbrace{\sum_{j=1}^{2} \frac{f_j\omega_{oj}^2}{\omega_{oj}^2 - \omega^2 + i\gamma_j\omega}}_{\text{Additional oscillators}} \quad (4)$$

The Classical dispersion model is based on the sum of a single and double Lorentzian, and Drude oscillators. Lorentz oscillator works well for transparent dielectric materials (Γ_0=0) or weakly absorbing materials ($\Gamma_0 \neq 0$). ε_∞ is the high frequency dielectric constant, ε_s is the static dielectric constant, ω_t (in eV) is the resonant frequency of the oscillator, and Γ_0 (in eV) is the broadening of the oscillator also known as the damping factor. Drude oscillator is an extension of the single Lorentz oscillator to the case of zero restoring force (ω_t = 0). This simple model is used to account for free electrons in metals and conductive oxides or, in the case of heavily doped semiconductors, free carriers. ω_p represents the plasma frequency where $\varepsilon_r(\omega)$ approaches zero and Γ_D is the collision frequency which describes the scattering of the electrons associated with electrical resistivity. Figure 2 shows the spectra of the refractive index (n, solid line) and extinction coefficient (k, dots) of the ITO film from 310 to 1240nm (1-4 eV).

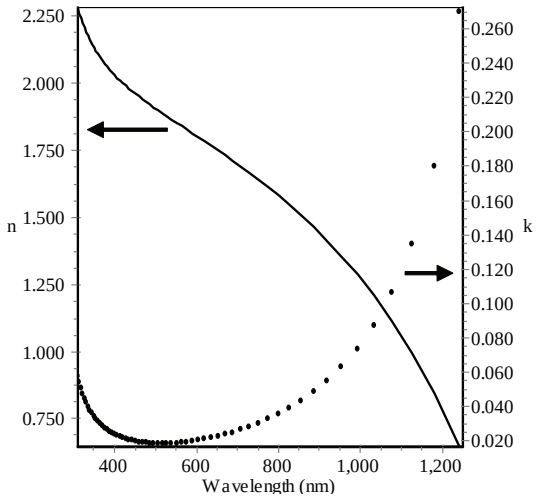

Figure 2: The refractive index (solid line) and extinction coefficient (dots) of the ITO film.

Glass/ITO/WO_3

Figure 3 shows the structure used to model this sample. The inclusion of a thin (22Å) interface layer between WO_3 and ITO improved significantly the goodness of fit (χ^2 decreased from 9.11 to 2.86). For brevity, only the SE raw data (combined with the model fits) from our final studied sample will be presented. As it turned out, the interface between ITO and WO_3 is oxygen deficient and can be described with an effective medium approximation (EMA) layer of 35.5% tungsten (W) plus 64.5% WO_3. The optical properties of the ITO layer were assumed be to the same as previously, but its thickness was allowed to vary in the fitting. Both the thickness and optical constants of the WO_3 layer were fitted.

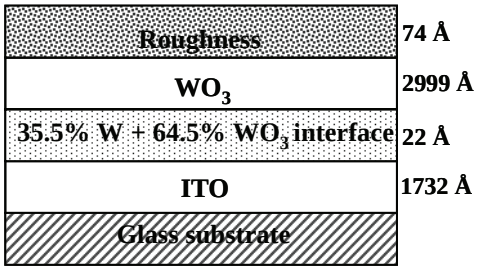

Figure 3: Structure used for modelling Glass/ITO/WO_3.

The optical functions of the tungsten oxide layer were parameterized using a new amorphous dispersion formula. Developed by HORIBA Jobin Yvon on the basis of Forouhi-Bloomer formulation [9], this model gives a Lorentzian shape to the expressions of the extinction coefficient and refractive index. The absorption coefficient is given by:

$$k_\omega = \begin{cases} \dfrac{f_j \cdot (\omega - \omega_g)^2}{(\omega - \omega_j)^2 + \Gamma^2} & \omega > \omega_g \\ 0 & \omega \le \omega_g \end{cases} \tag{5}$$

And the refractive index is written as such:

$$n(\omega) = n_\infty + \frac{B \cdot (\omega - \omega_j) + C}{(\omega - \omega_j)^2 + \Gamma_j^2} \tag{6}$$

where

$$\begin{cases} B_j = \dfrac{f_j}{\Gamma_j} \cdot \left(\Gamma_j^2 - (\omega_j - \omega_g)^2\right) \\ C_j = 2 \cdot f_j \cdot \Gamma_j \cdot (\omega_j - \omega_g) \end{cases} \tag{7}$$

ω_g (in eV) represents the energy band gap, f_j is related to the strength of the extinction coefficient peak, Γ_j is the broadening term of the absorption peak, and ω (in eV) is approximately the energy at which the extinction coefficient reaches its maximum. The new amorphous model works particularly well for amorphous materials exhibiting an absorption in the visible and/or far UV spectral range. The solid lines in Figure 4 are the extracted refractive index (n) and extinction coefficient (k) of the WO_3 film from 310 to 1240nm (1-4 eV). The crossed lines are the optical constants of the same material but from a separate sample (to be addressed in 3.5).

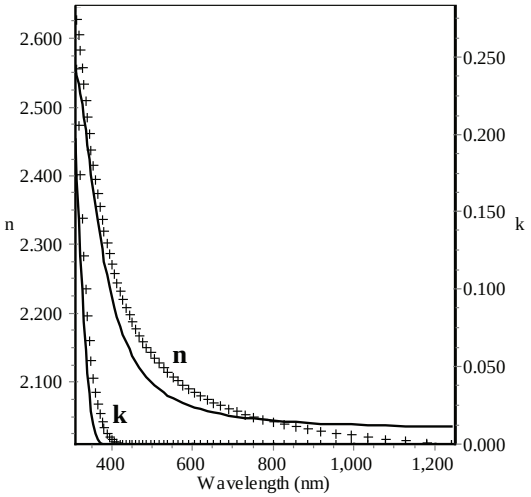

Figure 4: The refractive index (n) and extinction coefficient (k) of the WO_3 film extracted from two separate samples: Glass/ITO/WO_3 (—) and Glass/ITO/$TiVO_x$/Ta_2O_5/WO_3 (+++).

Glass/ITO/$TiVO_x$

The optical (and thereby electrochromic) properties of $TiVO_x$ thin films are strongly dependent on the film compositions and heat-treatment temperatures. Assuming the same ITO optical constants as above, the optical properties of $TiVO_x$ were extracted from this next sample using again a new amorphous dispersion formula. The thicknesses of both layers (ITO and $TiVO_x$) were fitted simultaneously with the dispersion parameters for $TiVO_x$. The final determined refractive index (n) and extinction coefficient (k) of the $TiVO_x$ film are shown in Figure 5 as solid lines. Also included are the extracted optical functions of the same but buried material from other samples (to be addressed next).

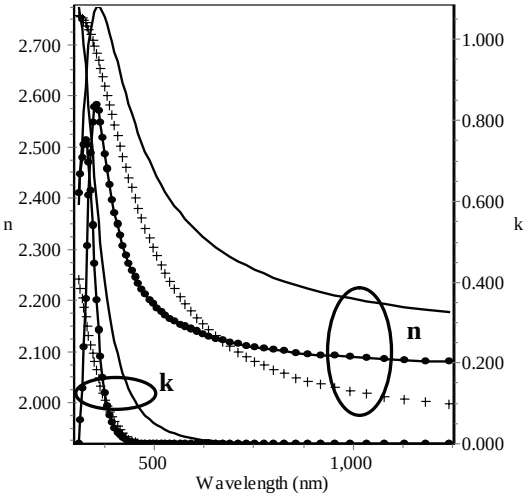

Figure 5: The refractive index (n) and extinction coefficient (k) of the $TiVO_x$ film extracted from three separate samples: 1) Glass/ITO/$TiVO_x$ (—); 2) Glass/ITO/$TiVO_x$/Ta_2O_5 (+++); and 3) Glass/ITO/$TiVO_x$/Ta_2O_5/WO_3 (-•-•-).

Glass/ITO/$TiVO_x$/Ta_2O_5

Built upon the previous sample, the Ta_2O_5 electrolyte film was characterized next assuming first the same optical properties and thicknesses for the underneath layers (ITO and $TiVO_x$) as obtained above. After this failed, a second attempt was followed allowing this time both the ITO and $TiVO_x$ film thicknesses to vary. Little was gained until the optical constants of the buried $TiVO_x$ layer were adjusted together with those of the outermost Ta_2O_5 layer.

The dielectric functions of Ta_2O_5 were parameterized using the absorbing Lorentz oscillator ($\Gamma \neq 0$ in Eqn. 4). The solid lines in Figure 6 show the as-determined refractive index and extinction coefficient of the Ta_2O_5 film from 310 to 1240nm (1-4 eV). The new set of $TiVO_x$ film optical constants are shown side-by-side in Figure 5 (crossed lines) with their starting values extracted from prior sample (solid lines). Though bearing much resemblance in terms of the dispersion (i.e., shape), there are clear shifts both in the peak position and amplitude. This indicates the pronounced effects of surroundings, neighboring films in this case, on the properties of this electrolyte material.

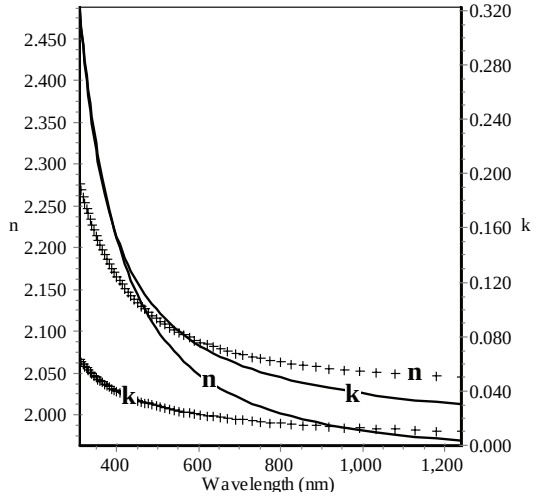

Figure 6: The refractive index (n) and extinction coefficient (k) of the Ta_2O_5 film extracted from two separate samples: Glass/ITO/$TiVO_x$/Ta_2O_5 (—) and Glass/ITO/$TiVO_x$/Ta_2O_5/WO_3 (+++).

Glass/ITO/$TiVO_x$/Ta_2O_5/WO_3

Built still upon the above sample, the final studied film stack includes all the constituent materials in the actual electrochromic device. As with previously, several modeling attempts would be made, starting with the simplest case scenario where all the layers buried below WO_3 were assumed to be the same as the last sample. Slowly, we would add as additional fit parameters first the thicknesses of $TiVO_x$ and Ta_2O_5, then the optical constants of Ta_2O_5, and finally the optical constants of $TiVO_x$ as well. The overall goal was to build, upon the information acquired already from prior measurements, a simplest model possible with fewer fit parameters which would yield unambiguous and physical results.

Figure 7 shows the final fit agreements (χ^2 ~3.6) between the experimental (dots) and model generated (lines) I_s and I_c data. The modified optical constants of the WO_3, $TiVO_x$, and Ta_2O_5 layers are shown separately in Figures 4 (crossed lines), 5 (dotted lines), and 6 (crossed lines), together with those extracted from the proceeding samples. The index evolutions for all three materials are clearly seen.

By measuring five separate samples with step-wise layer constructions, we were able to monitor very closely the development of each layer as the multi-layered EC structure is built up. The type of substrates obviously is important as it influences directly the nature of the film deposition process. Still, even with the same substrate and same deposition conditions, a deposited film may end up having distinctly different properties because of the layer(s) deposited subsequently atop.

For the $TiVO_x$ layer in this final studied sample, the definition of sandwiching layers goes beyond its immediate neighbors (ITO and Ta_2O_5) and includes also WO_3.

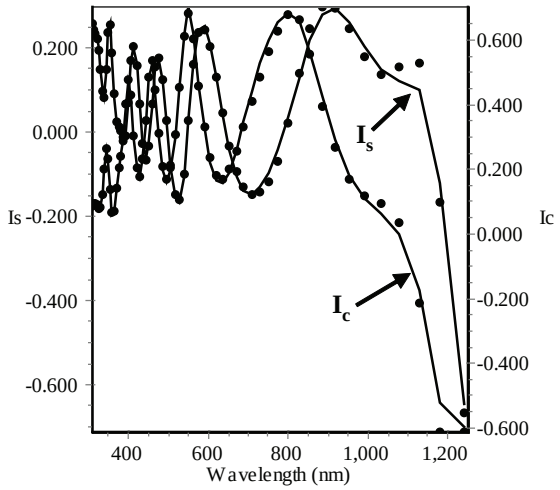

Figure 7: The fit agreements between the experimental (• • •) and best-fit model generated (—) Is and Ic data from Glass/ITO/$TiVO_x$/Ta_2O_5/WO_3.

CONCLUSIONS

A complete electrochromic device, Glass/ITO/$TiVO_x$/Ta_2O_5/WO_3/ITO/Glass, was characterized using the UVISEL phase modulated spectroscopic ellipsometer. Measurements were carried out on five separate samples with step-wise layer constructions. Results showed very clearly the film index shifts as a result of the progressively changing environment within a multi-layered stack. The detection of such index changes were made possible owing to the unparallel high accuracy and sensitivity of the PMSE technology in measuring multiple thin films on transparent substrates.

REFERENCES

1. C.G. Granqvist, *Handbook of Inorganic Electrochromic Materials*, Elsevier, Amsterdam, 1995.

2. C. Lampert, in *Large-Area Chromogenics: Materials and Devices for Transmittance Control*, ed. by C. Granqvist, Optical Engineering Press, Bellingham, 1990.

3. P.M.S. Monk, R.J. Mortimer, and D.R. Rosseinsky, *Electrochromic Fundamentals and Applications,* VCH, Weinhem, 1995.

4. B.W. Faughnan, R.S. Crandall, and P.M. Heyman, *RCA Rev.* 36, 177, 1975.

5. K. Yamanaka, H. Okamoto, H. Kidou, and T. Kudo, *Jpn. J. Appl. Phys.* 25, 1420, 1986.

6. R. M. A. Azzam and N. M. Bashara, *Ellipsometry and polarized light*, North-Holland, New York, 1977.

7. J. Humlíček, in *Handbook of ellipsometry*, ed. by H. G. Tompkins and E. A. Irene, William Andrew Publishing, New York, p. 77, 2005.

8. B. Drevillon, J. Y. Parey, M. Stchakovsky, R. Benferhat, Y. Josserand, and B. Schlayen, "Design of a New In-Situ Spectroscopic Phase-Modulated Ellipsometer," *SPIE Proc.*, 1188, 174, 1990.

9. A.R Forouhi and I. Bloomer, "Optical Properties of Crystalline Semiconductors and Dielectrics," *Phys. Rev.*, **B38 (3), 1865, 1988.**